EFDA–JET–PR(07)15

A.V. Krasilnikov, D. Van Eester, E. Lerche, J. Ongena, J. Mailloux, V.N. Amosov,
T. Biewer, C. Crombe, G. Bonheure,S. Jachmich,Yu.A. Kaschuck, V. Kiptily,
H. Leggate, M.-L. Mayoral, S. Popovichev, M. Santala, M. Stamp,
V. Vdovin, A. Walden and JET EFDA contributors

Ion Cyclotron Resonance Heating of JET Deuterium Plasma at Fundamental Frequency

Ion Cyclotron Resonance Heating of JET Deuterium Plasma at Fundamental Frequency

A.V. Krasilnikov[1], D. Van Eester[2], E. Lerche[2], J. Ongena[2], J.Mailloux[3], V.N.Amosov [4], T.Biewer[3], C.Crombe[3], G.Bonheure[3],S.Jachmich[3],Yu.A. Kaschuck[4], V. Kiptily[3], H. Leggate[3], M.-L. Mayoral[3], S. Popovichev[3], M. Santala[3], M. Stamp[3], V. Vdovin[4], A. Walden[3] and JET EFDA contributors*

JET-EFDA, Culham Science Centre, OX14 3DB, Abingdon, UK

[1]SRC RF Troitsk Institute for Innovating and Fusion Research, Troitsk, Russia,
[2]Laboratory of Plasma Physics – Association EURATOM – Belgian State - ERM/KMS, Trilateral Euregio Cluster, Brussels, Belgium,
[3]EURATOM-UKAEA Fusion Association, Culham Science Centre, OX14 3DB, Abingdon, OXON, UK
[4]RNC Kurchatov Institute, Nuclear Fusion Institute,Moscow, Russia,
** See annex of M. Watkins et al, "Overview of JET Results ", (Proc. 21st IAEA Fusion Energy Conference, Chengdu, China (2006).*

Preprint of Paper to be submitted for publication in Proceedings of
Zvenigorod
(Zvenigorod, Russian Federation, 12th February 2007)

ABSTRACT

The possibility to apply the Ion Cyclotron Resonance Heating (ICRH) scheme with fundamental heating of the majority ions in tokamak plasmas is of significant scientific and practical interest. The subject is especially important for the understanding of its perspectives in ITER DT plasma.

Results of the experimental studies of ICRH at the fundamental frequency of the majority deuterons in JET plasmas with near-tangential deuteron neutral beam injection (NBI) are presented. 1D, 2D and 3D modeling of JET plasmas ICRH were performed before the experiments with the application of TOMCAT, CYRANO and PSTELION codes, respectively. This modeling indicated that several ITER relevant mechanisms of heating may occur simultaneously in this heating scheme: fundamental ion cyclotron resonance heating of majority D ions, parasitic impurity ion heating and electron heating due to Landau damping and TTMP. All these mechanisms were studied in JET experiments with a ~90%D, 5%H plasma including traces of Be and Ar. Up to 2MW of ICRH power was applied at 25MHz. Dipole phasing was adopted, most power being launched with $|k_{||}| = 6.6m^{-1}$. All experiments were performed with $I_p = 2MA$, $n_e(0) = 2.5\times10^{19}\ m^{-3}$ and $R_{ax} = 2.97m$. In most of the discharges the toroidal magnetic field strength was 3.3T (plasma deuterons resonance layer at R=3m, Be and Ar resonances at 2.69 and 2.72m, respectively), but in one it was equal to 3.6T (plasma deuterons resonance layer at R=3.27m, Be and Ar resonances at 2.96 and 2.99m, respectively). Experiments were performed both with nearly tangential (~60^o with respect to the magnetic axis) as well as nearly perpendicular (~80^o with respect to the magnetic axis) neutral beam injection, and either using 130keV or 80keV beams. Approximately 5MW of beams were used, not only to preheat the bulk plasma, but also because fast deuterons have their cyclotron resonance Doppler shifted away from the cold resonance at which E_+ – the RF electric field component that governs ion heating - is small, the shift of the resonance yielding enhanced RF power absorption efficiency.

The effect of fundamental ICRH was demonstrated in these experiments at JET. Direct ICRH of fast beam deuterons was measured by the neutral particle analyzer in the energy range 120-240keV and was also noticed by g-spectroscopy. Electron and ion heating (directly by waves and indirectly by collisional relaxation of resonant deuterons) was observed by several diagnostics. It caused an ion and electron temperature increase from T_i~ 4.3 and T_e ~4.5keV (NBI-only phase) to T_i ~ 5.5 and T_e ~4.8keV (ICRH+NBI phase), respectively. Comparing energies and heating powers, no significant confinement degradation was observed during ICRH for the adopted RF power levels. By adding 23% of heating power ($P_{ICRH} = 1.6MW$ / $P_{NBI+OH} = 7MW$) the fusion power was increased at least by 35% due to ICRH.

1. INTRODUCTION

A well known advantage of Ion Cyclotron Resonance Frequency (ICRF) heating of plasma in future fusion reactors, including ITER, is the dominant ion heating leading to higher Q gain and possibilities for efficient driven burn control. JET practically has a reactor-like ICRF heating complex.

In most present-day tokamaks and stellarators, the preferred plasma heating scenario is the resonant

interaction of externally launched waves with a relatively small concentration ("minority") of resonant ions that efficiently absorb ICRF power at their fundamental cyclotron frequency and redistribute it due to the drag of the energetic minority tail on electrons and bulk ions. As it necessitates a minority gas being immersed in another bulk ion gas, this scheme of heating was called "minority" ICRH. It will be used in ITER's non active hydrogen phase with D^+, $^3He^{2+}$ and $^4He^{2+}$ as minority ions. In the activated deuterium – tritium ITER phase the concentration of the two reacting ions (D and T) is not small. For that phase, it was proposed to adopt second harmonic tritium heating, using a wave absorption mechanism resting on finite ion Larmor radius effects. As tritium second harmonic heating currently is the only RF heating scheme proposed for the activated ITER phase, it seems worthwhile to examine the potential of a supplementary scheme, in particular one that heats the second fuel ion species in a fusion reactor relying on D-T fusion.

Ion heating schemes at the fundamental cyclotron frequency of the majority ions were tested in the past. There were successful experiments in the stellarator-C (1968, PPPL), the Kharkov torsatrons and the US mirror traps. Small tokamaks (TM-1-Vch (1974) [1], TO-2 [2] in RRC "Kurchatov institute", T-11M [3] in SRC RF TRINITI and Globus-M [4] in "Ioffe institute") also have shown good heating results at the fundamental harmonic of the majority ions. It is important to note that the world's largest stellarator LHD, well equipped with diagnostics, has recently demonstrated bulk ion heating at the fundamental harmonic at high plasma densities close to those of scenarios foreseen for ITER's activated phase [5].

Non-negligible amounts of Beryllium (~2%) are expected to be present in ITER due to the use of Be limiters. Argon is under discussion for application in the ITER divertor for reirradiation of the power incoming into the divertor. In case some amount of Argon impurity will be used, it will undoubtedly penetrate ITER's main plasma. Beryllium nor Argon are deuterium-like ions (Z/M= 4/9 and 9/20, respectively) and therefore have their ion cyclotron layer shifted away from that of the D bulk ions. Bulk ion heating was also demonstrated in experiments with fundamental deuterium ICRH in 20% D + 80% T plasma during DTE1 [6]. One of the possible mechanisms of bulk ion heating in those experiments was resonant absorption of the RF power by Be impurities, the concentration of which was estimated to be 1.5% in those experiments. ICRH of Be and Ar traces was purposely studied in our recent experiment to find out if this indirect heating indeed contributes to bulk ion heating.

Studies of the fundamental ICRH mechanism in ITER-like conditions at JET are crucial for understanding the perspectives of application of this ICRH scheme in ITER D-T plasmas.

The results of experimental studies and mathematical modeling using 1D, 2D and 3D full wave ICRF codes of ICRF heating experiments of JET plasmas at the fundamental IC resonance of bulk plasma ions in conditions modeling the driven burn ITER plasma are presented in the present paper. Section 2 presents results of mathematical modeling. The experimental arrangement is shown in Section 3. The main results of JET fundamental ICRH presented in Section 4 and conclusions summarized in Section 5.

2. NUMERICAL MODELING OF JET ICRH AT FUNDAMENTAL FREQUENCY

Intensive modeling was carried out for JET experimental conditions before, during and after the experiments. For 1-, 2- and 3-D estimates of the RF power absorption on ions and electrons, the TOMCAT [7], CYRANO [8] and PSTELION [9] codes were respectively used. The first two codes rely on finite element modeling while the third one on centered difference descretization, and differ in some details of the physics model and its numerical implementation. The 1-D model retains up to second order Finite Larmor radius effects in the operator acting on the field as well as on the test function in the variational formulation of the problem and hence contains up 4^{th} order Finite Larmor Radius (FLR) terms in the equivalent dielectric tensor, allowing to describe Landau and TTMP damping as well as cyclotron heating up to the third cyclotron harmonic by a wave model accounting for 12 independent modes. It accounts for the toroidal curvature of the machine but – by definition – does not account at all for the – important - geometry-related effects. These effects are fully accounted for both in CYRANO and PSTELION, the latter code equally enabling the study of stellarator plasmas as it is a full-3D code. Both CYRANO and PSTELION rely on a Fourier expansion of the RF fields and test function in the poloidal direction and retain up to second order FLR effects in the equivalent dielectric tensor i.e. describe the evolution of 6 hot plasma modes. Both in CYRANO and PSTELION, actual JET equilibria can be imported.

All simulations were performed for similar plasma content: majority D (thermal + beam) ions, ~5% H and traces of Be, C and Ar. Other parameters of JET fundamental ICRH experiments used in simulations were the following: Density $n_e = 2.5\times10^{19}$ m^{-3}, temperature $T_e = T_i = 5.5$keV, magnetic field strength on axis $B_{ax} = 3.3$T, neutral beam power $P_{NBI} = 5$ MW and energy $E_{NBI} = 130$keV, ICRH power $P_{ICRH} = 2$MW, frequency $f_{ICRH} = 25$MHz and phasing N = +27 (dipole).

The distribution of the power absorption calculated by the 1D TOMCAT code under assumption that all deuterons (86%) are thermal is presented in Fig.1 and the integrated powers are given in Table 1. According to TOMCAT code modeling, most of the power absorbed by thermal plasma power is absorbed by electrons (61%) and deuterons (31%), the fraction going to the electrons decreasing as the ion temperature is increased or when beams are accounted for (a beam with a concentration of 10% and modeled as a 50keV Maxwellian yields a roughly balanced absorption between electrons and D ions). As the TOMCAT code is commonly run excluding the low field side antenna region, it is able to compute the outgoing wave fluxes and power deposition consistent with an incoming wave flux. The code predicts a very low ~ 5% total double pass power absorption suggesting that large electric fields are likely to be set up in order to absorb the launched power and hence that interaction with the wall can be expected to be significant, as was observed in the experiment.

The two-dimensional CYRANO code was also used to study the fate of the RF power for the fundamental ICRH scheme for the above mentioned JET experimental conditions, taking into account the wave absorption by fast beam deuterons for various beam concentrations. The simulations made by the 2D CYRANO code took into account up to 80 poloidal modes, which gives a good description of the wave dynamics as long as mode conversion is not important. Noting short wavelength structure

is almost absent in Fig.1 (the only short wavelength structure appears locally at the Be-related ion-ion hybrid layer) this seems a reasonable approximation although confirmation is clearly needed (and provided by PSTELION, as is discussed next) using many more modes. Fast beam deuterons were represented by an isotropic Maxwellian distribution with effective temperature of 50 keV. Results of calculations of the distribution of the power absorbed by various plasma particles are presented in Fig.2. The calculated power partitioning between plasma components for 2 different beam concentrations are also presented in Table 1. One of the main results of the 2D simulations with the CYRANO code is that most of the power (95%) is roughly equally shared between electrons and D ions, and that beam D RF absorption exceeds thermal D absorption for beam concentrations of the order of 20%. Only the remaining fraction (5%) is shared among the various impurities.

The three-dimensional full wave code PSTELION, finally, was equally applied for modelling ICRH at the fundamental frequency of JET majority plasma and beam injected deuterons simulation. The effect of the Doppler shift of the resonance layer position of the fast beam deuterons injected at an angle of 60^0 with respect to the magnetic axis was addressed in particular. Fast beam deuterons were described by a Maxwellian distribution with effective temperature 52 keV shifted in the $v_{//}$-direction in velocity space. It was in particular shown that fast deuterons having low field side Doppler shift of the resonance layer position are absorbing the ICRF wave power more efficiently than those having a high field side Doppler shift as expected from the position of the fast wave cut-off. As up to 1000 poloidal modes were taken into account, the calculations made by the 3-D PSTELION code not only allow to study the fast wave dynamics but equally the fate of power transferred at ion-ion hybrid layers to mode converted short wavelength branches (IBW and ICW) in the actual geometry. Distribution of the power absorbed by various plasma particles calculated taking into account fast perpendicular injected beam deuterons modeling by a Maxwellian distribution with effective temperature 52 keV is presented in Fig.3. To study the dependence of the various heating mechanism efficiencies on the position of the various resonating ion resonance layer positions the simulations were performed for both the values of the JET axial magnetic field strength actually applied in experiments, 3.3 and 3.6 T. The simulations suggest that the location of the absorption layers and the amount of impurity ions play an important role in the RF power partitioning. In particular, the radial profiles of the power absorbed by the ions differ significantly for different magnetic field strengths (compare Figs.3a and 3b). Increasing the Ar concentration from 0.1% to 0.5% at 3.6T clearly leads to enhanced Ar absorption (compare Figs. 3b and 3c). The predicted power partitioning between plasma components is also presented in Table 1.

The simulations made by the various adopted wave codes have all confirmed that electron damping is significant in the majority D-heating JET scenario. Majority D heating and – particularly beam D heating – evidently plays a key role, but also traces of impurities have a possible impact on the predicted absorption that should not be overlooked.

3. FUNDAMENTAL ICRH EXPERIMENT ARRANGEMENT

The main goal of the experiment was the study of the efficiency of the interaction of ICRF waves with the majority deuterium ions in conditions relevant for reactor (ITER) D-T plasmas. In particular, the following heating mechanisms were foreseen as the results of predictive modelling: fundamental ICRH of bulk D-plasma (pre-heated to higher than Ohmic temperatures by high energy deuterium neutral beam injection), fundamental ICRH of beam D ions (benefiting from the enhanced Doppler shift), indirect ICRH of bulk D-plasma through controllable addition of Beryllium and Argon, and direct electron heating. Be and Ar being fairly massive guarantees that the power they absorb is rapidly transferred to the bulk ions by collisions.

All mechanisms were studied in JET experiments with plasma containing ~90% D, 5% H, as well as main impurities Be (~1%, with decreasing concentration from shot to shot after vacuum vessel beryllium evaporation prior to the experiments) and Ar (≤0.5% due to gas puff). The experiments were performed with I_p = 2 MA, $n_e(0) = 2.5\times10^{19}$ m^{-3} (optimized to favor RF heating of the beam ions) and R_{ax} = 2.97 m. To avoid sawteeth the current diffusion was influenced by application of 1.7 MW of lower hybrid heating at the beginning of the discharge. Two sessions of experiments were carried out. The first was performed with 5MW of low energy (80keV) NBI injected from octant 4 at about ~80^o to the magnetic axis (normal beam) and 1.3MW, 130keV beam injected at ~60^o (tangential beam) to magnetic axis. The second experiment adopted 5.9MW of 130keV beam, integrally injected from octant 8 at ~60^o to the magnetic axis (see Fig.4). The NBI power was limited to avoid going into H-mode. Up to 1.65 and 2MW of ICRH power were applied at 25MHz during the first and second sessions, respectively. To optimize heating, dipole phasing was imposed, most power being launched with $|k_{||}| = 6.6\ m^{-1}$. As mentioned above, the experimental conditions were chosen to have the peak of the beam ions density profile approximately coinciding with the position of the Doppler shifted resonance of the energetic beam particles $\omega = \omega_{cD} - k_{||}v_{||}$. In most of the discharges the toroidal magnetic field strength was equal to 3.3T (the plasma deuterons resonance layer is at R = 3m, Be and Ar resonances are at 2.69 and 2.72m, respectively). One experiment required using 3.6T (the deuteron resonance layer then is at R = 3.27m while the Be and Ar resonances are at 2.96 and 2.99m, respectively). The dependence of the resonance layer position along the plasma major radius as function off the magnetic field strength at the axis is shown for various ions in Fig.5.

To study the mechanisms of fundamental ICRH in detail, a number of non-standardly used diagnostics were exploited: The high energy perpendicular Neutral Particle Analyzer (NPA) adjusted for charge exchange deuteron atom energy distribution measurements in the range 0.1–1MeV, perpendicular and tangential neutron compact spectrometers of NE-213 and Stilbene detectors, the vertical neutron-time-flight spectrometer TOFOR1, the radial and vertical neutron cameras, gamma spectrometers. Values for the electron temperature $T_e(r)$ and density $n_e(r)$ are routinely provided at JET but the bulk ion temperature $T_i(r)$, as well as the density and temperature of impurities such as Be require dedicated CXRS measurements.

4. RESULTS OF ICRH AT FUNDAMENTAL FREQUENCY OF MAJORITY DEUTERONS AT JET

As was mentioned in the previous section, the first session of experiments (Pulse No's: 68282-68290) was carried out with 5MW perpendicular and 1.3MW tangential beam injection. The maximal ICRH power reached was 1.65MW (in Pulse No: 68288). The second session of experiments (Pulse No's: 68729-68734) was carried out with 5.9MW tangential beam injection. The maximal ICRH power (2 MW) during this session was reached in Pulse No's: 68733 and 68734.

Evolutions of plasma stored energy, central electron temperature measured by LIDAR and total neutron yield measured by fission chamber together with NBI and ICRH powers in discharge 68287 are presented in Fig.6. The effect of ICRH on plasma stored energy, electron temperature and total neutron yield is visible in Fig.6 at all values. In particular, fusion power increases by 45% when only ~20% of heating power was added by RF. About 35% of this fusion power increase is due to ICRH.

All discharges contained a phase during which only NBI was present, a phase during which RF and beams sources were active and finished with an RF-only phase (but still with ~1.5MW of diagnostic beam power). The changes of the vertical and horizontal neutron camera signals due to these different heating sources are illustrated in Fig.7 for Pulse No's: 68288 and 68733. Note the synergistic effect: a given RF power level yields a stronger increase in the neutron yield when NBI power is present than when it is not, suggesting that the RF heating is benefiting from the "preheated" ions.

The effect of ICRF wave interaction with beam injected deuterons measured by high energy perpendicular NPA is shown in Figs.8 and 9. The NPA measured the energy distributions of CX deuterium atoms leaving the plasma perpendicular to the magnetic axis in the equatorial plane. During ICRH a subpopulation of beam deuterons is accelerated to energies significantly higher than the beam injection energy; the magnitude of this energy change increases with ICRH power. Measured by NPA in the energy range 120-240keV effective perpendicular temperatures of fast deuterons reach values of about 50keV during the combined NBI+ICRH phase in Pulse No's: 68288 and 68733. By comparing the NPA spectrum obtained for shot 68733 in the NBI+RF phase [47-48s] and that obtained in the NBI-only phase [9.2-50s], the effect of the slowing down of the ICRH accelerated deuterons after the ICRH has been switched off is clearly observed (Fig.9).

It should be mentioned that none of the compact -neutron spectrometers-NE-213 with horizontal perpendicular sighting line and the Stilbene with tangential) view measured any major change in the *shape* of the D-D neutron energy distribution due to ICRH. It was found that the distribution of the deuterons in the 5-100keV suprathermal energy range is mostly determined by slowing down of fast beam deuterons and is not significantly altered by the application of a - limited - amount (maximally 2MW) of ICRH power. It was, however, equally observed that the neutron yield not only depends on the ambient bulk temperature but also on the applied RF power level. Both effects point in the direction of the beneficial synergistic "pre-heating" effect discussed in Fig.7.

The effects of fundamental ICRH onto plasma electron and ion temperatures are presented in Fig.10 for Pulse No: 68733 with 5.9MW, 130keV tangential NBI. One clearly sees the response of

the ion and electron temperature signals to the RF waveform. Temperature increases up to DT_i = 0.8keV and DT_e = 0.4keV were achieved near the plasma center when adding 2MW of RF power. Both electron and ion temperatures decrease in the outer plasma region during ICRH start-up, an effect attributed to the strong impurity influx from the wall into the plasma. After t~0.5s, this effect fades out but both the electron and ion temperature profiles remain somewhat peaked during most of the RF phase (see Fig.12); this peaking, which is localized in the plasma centre (r< 0.25m), is consistent with on-axis RF heating.

To compare experimentally the relative efficiency of on- versus off-axis majority D heating as well as impurity absorption in JET, Pulse No: 68734 was done at a different magnetic field, 3.6T instead of the otherwise used field strength of 3.3T. The ICRH resonance layers moved as follows: for plasma deuterons from 3.0m (on-axis) to 3.27m (off-axis), for Be and Ar impurities from 2.69 and 2.72m (off-axis) to 2.96 and 2.99m (on-axis). Compared to the on-axis heating pulses (e.g. Pulse No: 68733), a broadening of both the ion (Fig.11) and the electron (Fig.12) temperature profiles was observed. No convincing changes in fast perpendicular NPA atomic spectra and neutron source profiles were measured in these discharges.

CONCLUSIONS AND FUTURE PROSPECTS

ICRH of majority D ions was studied at JET. Direct heating of thermal D ions proved difficult at the available RF power levels but "preheated" fast beam injected deuterons seemed – as theoretically predicted – to profit from the combined effect of NBI and ICRH at fundamental deuterium frequency. ICRH of a subpopulation of the beam ions was measured by NPA in the energy range 120 - 240keV and was also noticed by g-spectroscopy.

Electron and bulk thermal ion heating (directly by wave and indirectly by collisional relaxation of resonant deuterons) was measured during ICRH. It caused ion and electron temperature increases from T_i = 4.3kev to 5.5keV and from T_e~4.5keV to T_e~4.8keV. From the comparison of the ion and electron temperature profiles measured during discharges with D, Be and Ar resonances at 3.0m, 2.69m and 2.72m (B_0 = 3.3T) and D, Be and Ar resonances at 3.27m, 2.96m and 2.99m (B_0 = 3.6T) it was concluded that in performed JET experiments the mechanism of heating through direct deuterium wave absorption is more efficient than those through wave absorption by Be and Ar impurities.

No confinement degradation was observed during ICRH at the available RF power levels. The heating efficiency during ICRH was similar to that in the NBI+Ohmic heating phase. Considerable impurity influxes from the wall were measured during ICRH, suggesting that – for the available JET configuration, e.g. the low RF frequency required to test D fundamental cyclotron heating - the adopted scheme has marginal single-pass absorption and thus leads to large electric fields, in particular in the edge.

By adding ~20% of heating power (P_{ICRH} = 1.5 MW/$_{PNBI+OH}$ = 7MW) the fusion power was increased by ~ 35% due to RF heating.

The experimental findings of the present work are in line with the theoretical insights. As the here

adopted scheme is predicted to be more promising on ITER because of the higher densities and temperatures, further experimental studies of majority deuteron heating are very important but require higher RF power (>3MW). Also the balanced H-^{3}He majority fundamental RF heating scenarii should be foreseen for future ITER-like JET ICRF experiments to model basic D-T ITER scenario and to contribute for the non-activated ITER phase. Such experiments will help build confidence that majority heating schemes can be optimized to heat ITER.

The confinement of fast beam injected deuterons and their spatial distribution could be a critical issue in ITER.

Beam ion confinement is thought to be degraded due to Alfvén eigenmode instabilities that are excited by strongly anisotropic beam deuterons and fusion alpha-particles. These instabilities could redistribute beam deuterons to the plasma periphery [11]. The ICRF-induced pinch could be used to affect the fast ion profile during heating [12]. RF heating can also be adopted to populate the region in velocity space between the thermal domain and the fast particle source, reducing the positive gradient of the distribution responsible for growth of MHD modes. Both these phenomena could be exploited in ITER to diminish the Alfven eigenmode instability drive related to fast ions, and must be addressed – e.g. during upcoming JET experiments – prior to ITER's first plasma.

REFERENCES

[1]. V.Vdovin et. al., "ICRH at fundamental frequency on TM-1-Vch tokamak" at IAEA Plasma Phys. And Contr. Fusion Conference 1974 (Tokyo).

[2]. Artemenkov L.I., Kovan I.A., Monakhov I.A, et al.. "Plasma heating at fundamental ion cyclotron frequency in the TO-2 tokamak", Plasma Physics and Controlled Nuclear Fusion Research, 1984, Proc. 10th IAEA Int. Conf., London, 12-19 Sept. 1984, IAEA, Vienna, 1985, Vol.1, p.615-621) see also: Amosov V.N. Artemenkov L.I., Kovan I.A., et.al., Sov.J. Plasma Physics, v.14 (5), p.363 (1988).

[3]. Maltsev S.G., Kovan I.A. et.al., "Fundamental ICRH of T-11M hydrogen plasma" in Proceedings of 20-IAEA Fusion Energy Conference (2004), see also: N.B.Rodionov, Azizov.E.A, Krasilnikov A.V. et.al., Sov. J. Plasma Physics, v.32 (2), p.1-11 (2006).

[4]. V.K.Gusev, et.al., "ICRF experiments on the spherical tokamak Globus-M" in Proceedings of 20-IAEA Fusion Energy Conference (2004)

[5]. T.Mutoh, R.Kumazawa, T.Seki, et.al., Nucl.Fusion **43**, 738-743 (2003)

[6]. D.F.H.Start et.al., Nuclear Fusion,v.**39**, No.3, p.321 (1999).

[7]. D. Van Eester and R. Koch, Plasma Phys. Contr. Fusion **40**, 1949-1975 (1998)

[8]. P.U. Lamalle, "Nonlocal theoretical generalisation and tridimensional numerical study of the coupling of an ICRH antenna to a tokamak plasma", PhD thesis, UniversitÈ de Mons, 1994 and LPP-ERM/KMS Report nr. 101.

[9]. Vdovin V.L. ICRF benchmarking modelling of ITER scenario #2, 7th Steady State Operation ITPA Topical Group meeting, Como, Italy, May 4-6, 2005

[10]. J. K‰llne et al., “Special Analysis of TOFOR data of JET Pulse No’s 68284 and 88288”, Uppsala University Neutron Physics Report 070219 (2007)
[11]. N.N.Gorelenkov, et.al. Nuclear Fusion v.**43**, p. (2003)
[12]. M.Mantsinen, et.al., Phys.Rev.Letters, v.**88**, n.11, p.115004 (2002)

[1] Results from the new TOFOR spectrometer will be presented in a ~~forth coming~~forthcoming paper exploiting the neutron emission spectroscopy (NES) diagnostic information available for some of the discharges studied here. [10]

Power (%) absorbed by → Absorbed power partitioning (%) predicted by:	Thermal D	Beam D	e	Be (1%)	Ar	C
1D TOMCAT – thermal plasma	31	0	61	2	3	3
1D TOMCAT – 10% beam D	22	27	46	Not simulated	3	2
2D CYRANO – thermal plasma	33	0	60	2	4	1
2D CYRANO - 10% fast beam D	27	18	49	1	3	1
2D CYRANO - 20% fast beam D	24	30	41	1	2	1
3D STELION with 5% fast D and B = 3.3T, Ar – 0.1%	24	7	65	3	<1	–
3D STELION with 5% fast D and B = 3.6T, Ar – 0.1%	42	6	37	12	2	–
3D STELION with 5% fast D and B = 3.6T, Ar – 0.5%	42	9	35	6	8.5	–

Table 1:

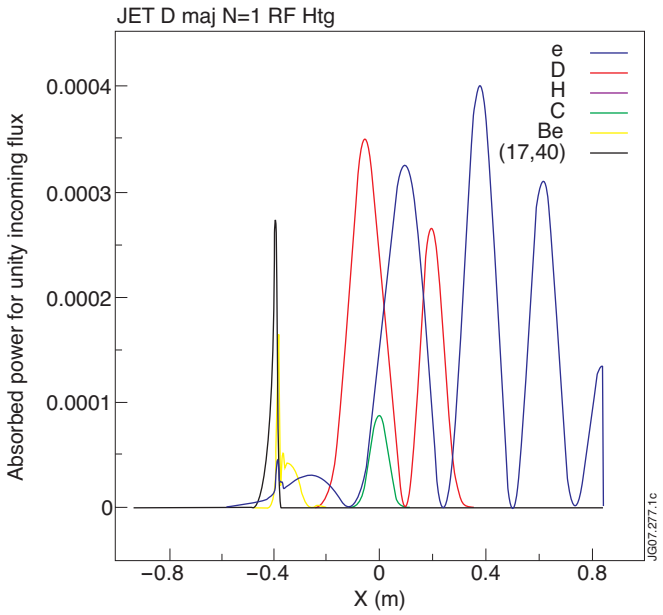

Figure 1: ICRH power density absorption profiles as simulated by the 1D TOMCAT code for JET experimental conditions.

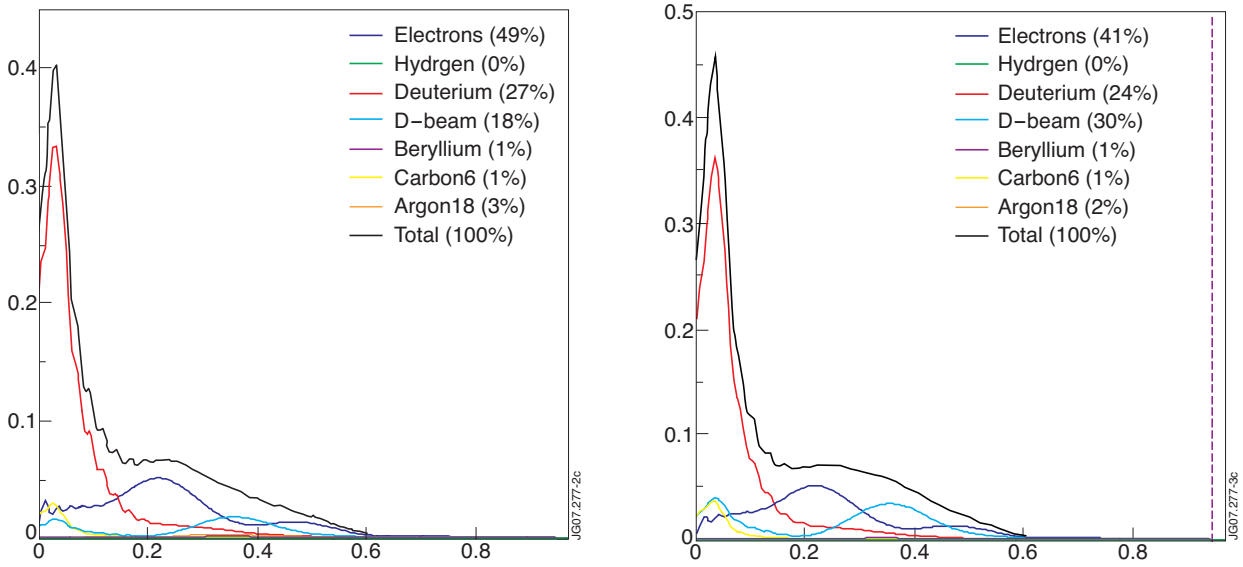

Figure 2: Distribution of fundamental ICRH power absorption simulated by 2D CYRANO code for JET experimental conditions; a) with 10% and b) with 20% of 50keV beam deuterons.

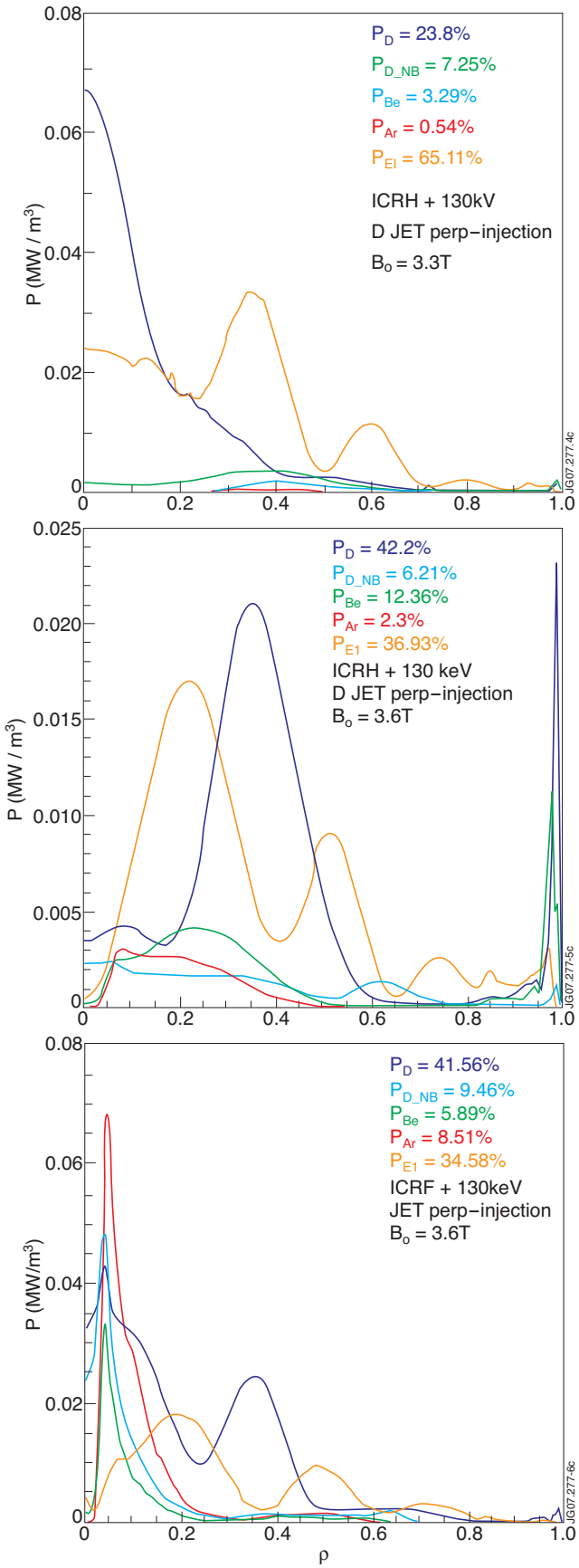

Figure 3: Distribution of fundamental ICRH power absorption simulated by 3D PSTELION full wave code for JET experimental conditions with $B_0 = 3.3T$ (a) and $B_0 = 3.6T$ (b,c) and Ar concentration equal to 0.1% (a,b) and 0.5% (c) taking into account absorption by fast beam deuterons.

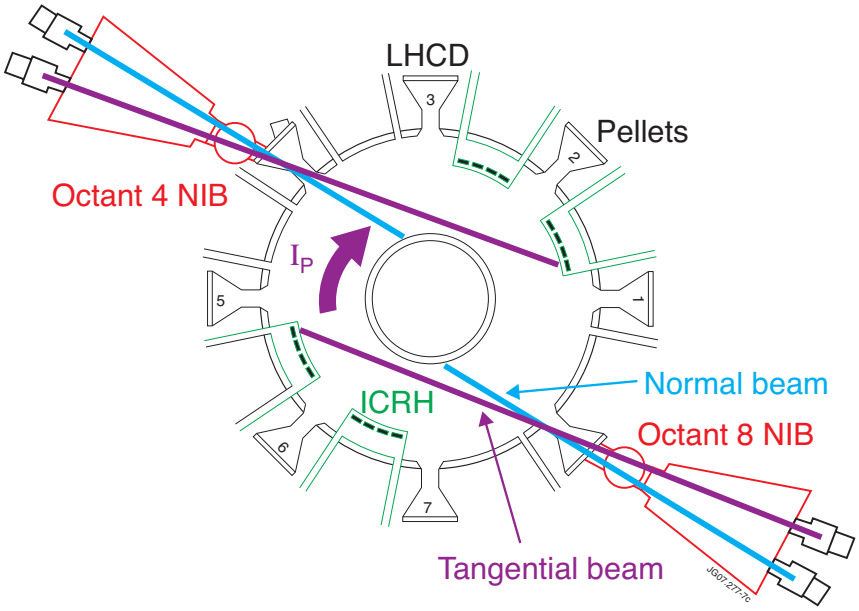

Figure 4: Arrangement of NBI and ICRH antennas at JET

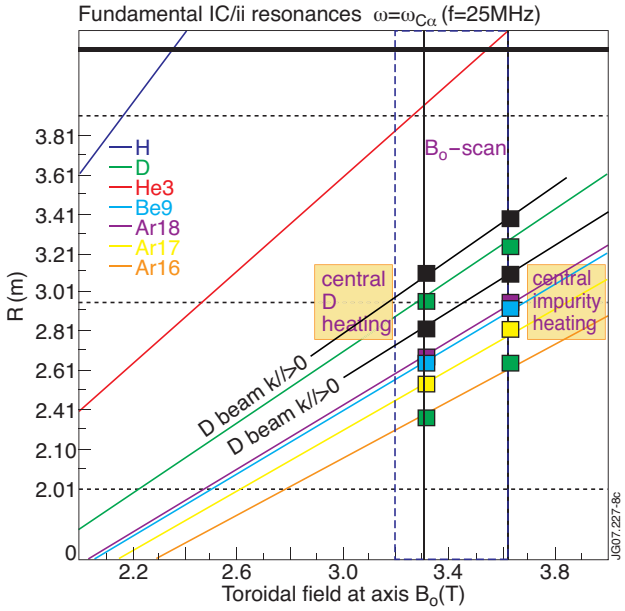

Figure 5: Fundamental ion cyclotron position dependence upon magnetic field at plasma axis for various JET plasma ions.

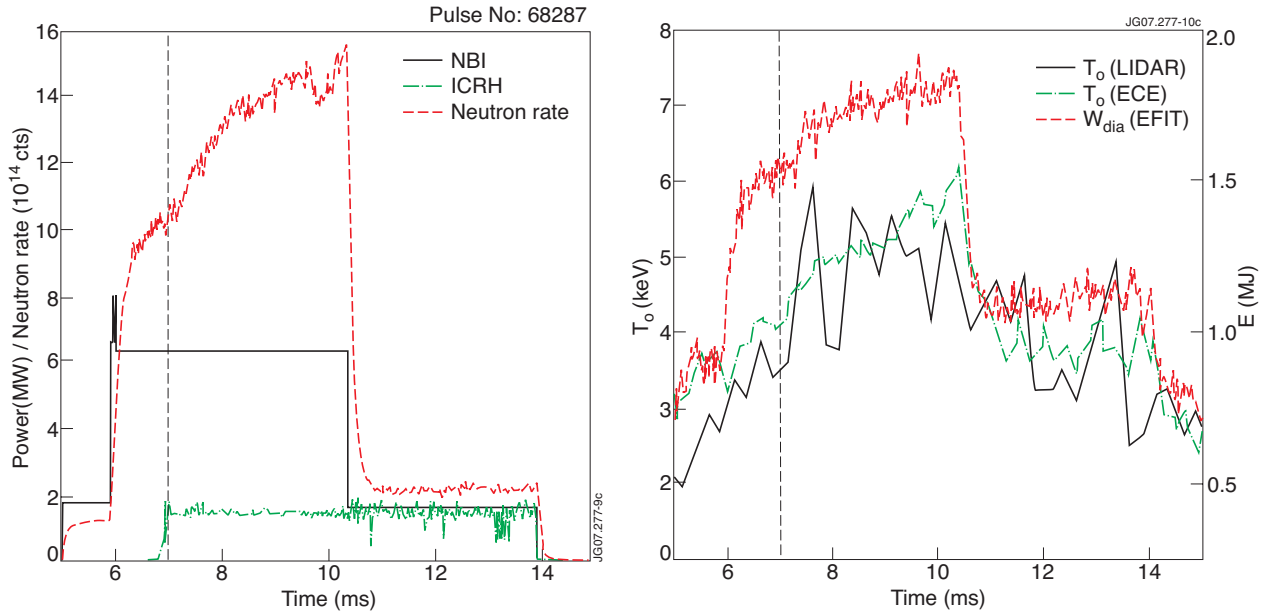

Figure 6: Evolutions of neutron rate, plasma stored energy (W_{dia}) and central electron temperature (T_0) together with NBI and fundamental ICRH powers in Pulse No: 68287.

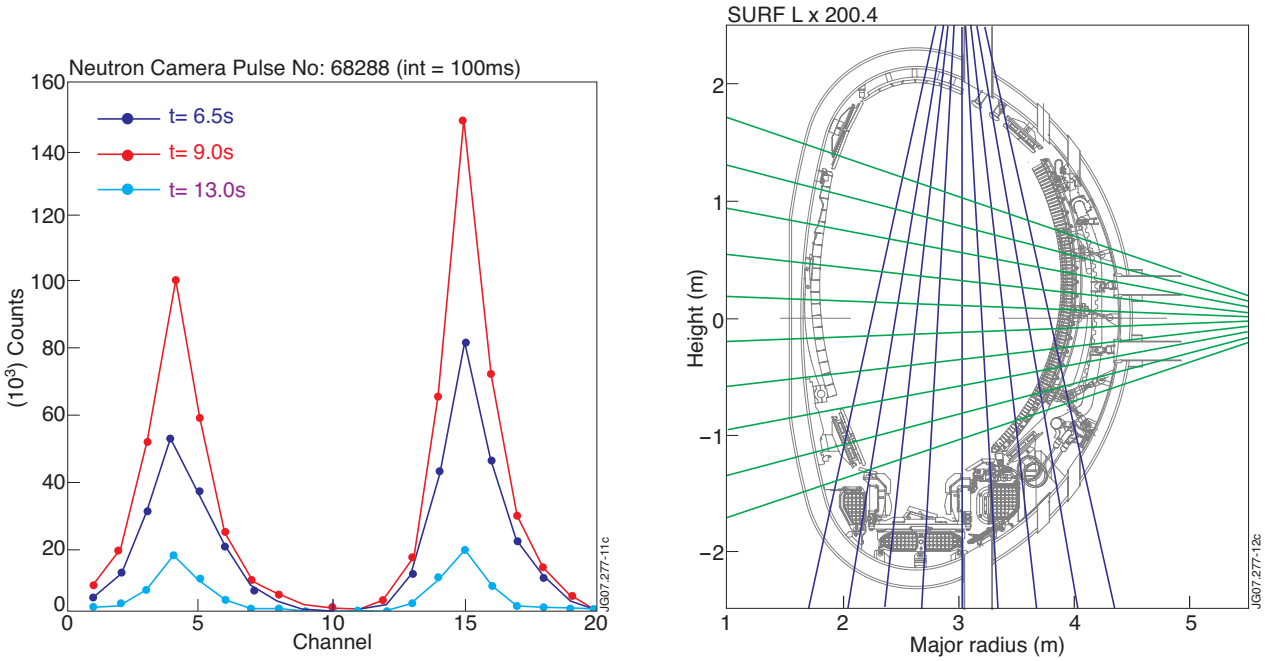

Figure 7(a): Neutron counts detected by horizontal (channel 1-10 from top to bottom) and vertical (11-19 from inward to outward) neutron cameras during shot 68288: neutron source profiles for time windows with 5MW perpendicular and 1.3 MW tangential NBI (red curve), same NBI together with 1.65 MW ICRH (green curve) and 1.3MW tangential NBI together with 1.65MW ICRH (blue curve). The lines of sight of the neutron camera are provided in the small figure on the right.

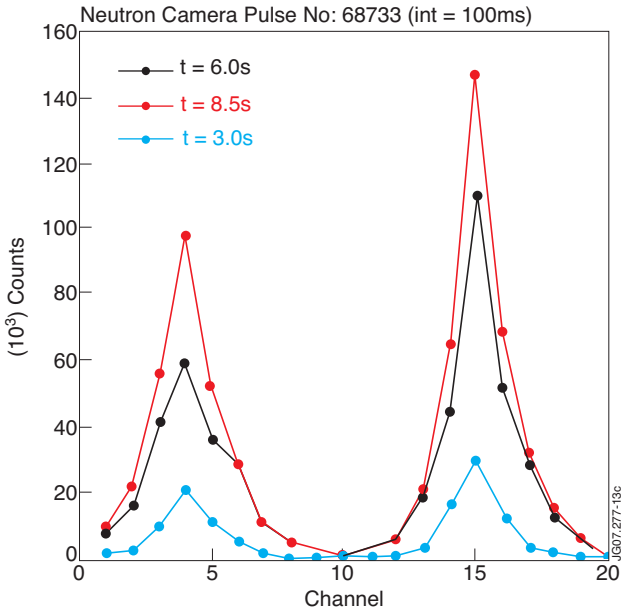

Figure 7(b): Neutron counts of the horizontal and vertical neutron cameras during Pulse No: 68733 neutron source profiles for time windows with 5.9MW tangential NBI (blue curve), same NBI together with 2MW ICRH (red curve) and 1.3MW tangential NBI together with 1MW ICRH (magenta curve). The channel numbers are as in Fig.7a.

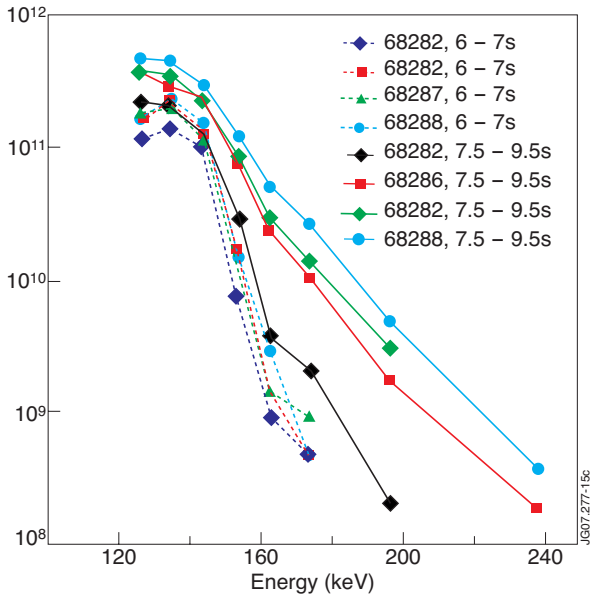

Figure 8: Integrated perpendicular fast CX deuterium atom spectra measured by NPA during various pulses in the NBI-only (time window 6.0-7.0s) and in the combined NBI + ICRH (7.5-9.5s) phases. The ICRH power was gradually increased in Pulse No's: 68282, 68286, 68287 and 68288 (P_{RF} = 0.5MW, 1.4MW, 1.45MW and 1.65MW, respectively).

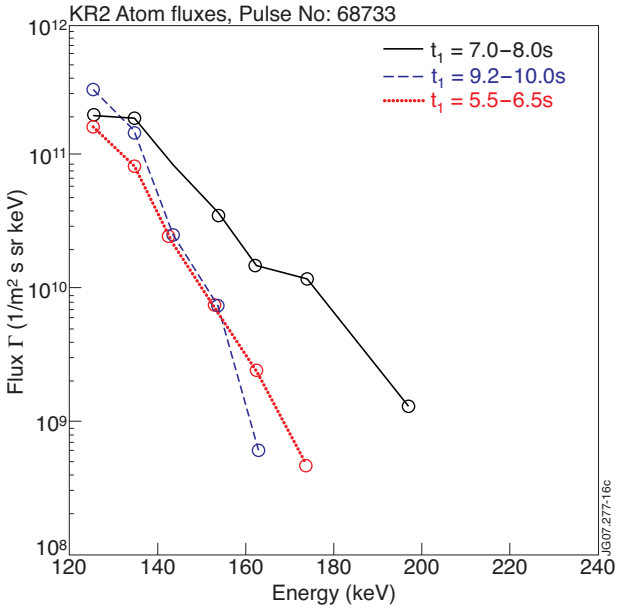

Figure 9: Perpendicular CX deuterium atom spectra measured by NPA during the NBI-only phases [5.5-6.5s] and [9.2-10.0s], and during the combined NBI+ICRH phase [7.0-8.0s] of Pulse No: 68733. In this pulse, 5.9MW of tangential 130keV beams and 2MW of RF power were applied.

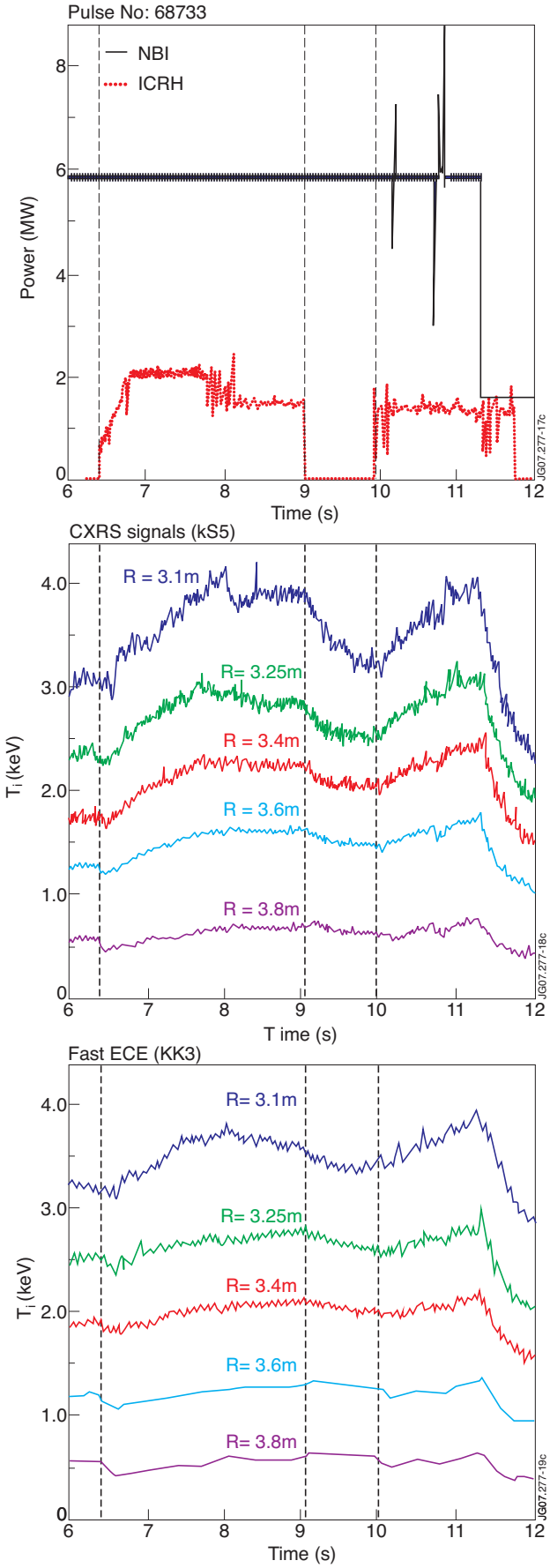

Figure 10: Evolution of the ion and electron temperature measured by CXRS and ECE diagnostics, respectively, for several major radii ranging from 3.1 to 3.8m, plotted with NBI and ICRH power in Pulse No: 68733

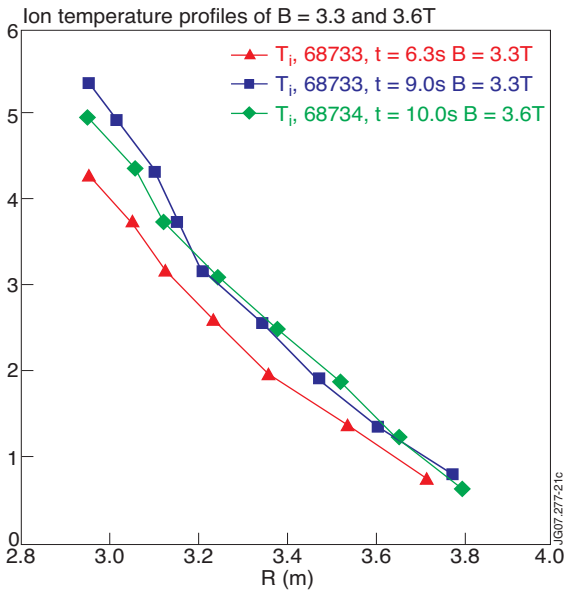

Figure 11: Ion temperature profiles measured by CXRS during 1.5MW ICRH at t = 9.0s in Pulse No: 68733 (B_0 = 3.3T; D, Be and Ar resonances at 3.0, 2.69 and 2.72m) and at t = 10.0s of 68734 (B_0 = 3.6T; D, Be and Ar resonances at 3.27, 2.96 and 2.99 m). The red curve shows the Ti profile during the NBI phase of Pulse No: 68733.

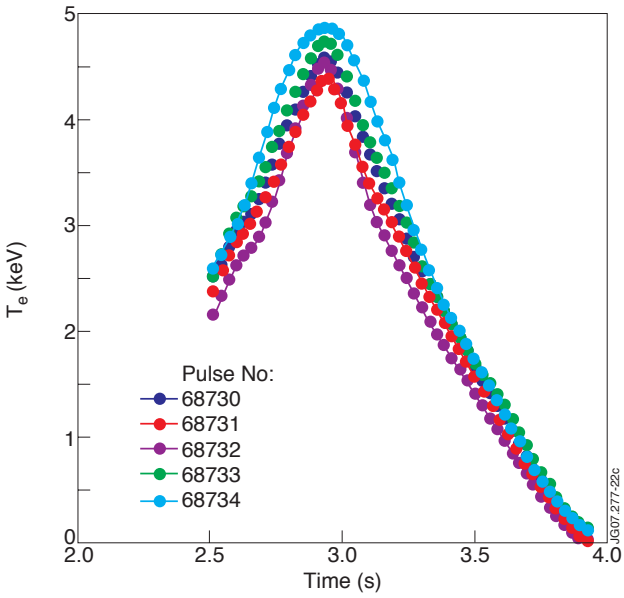

Figure 12: Electron temperature profiles measured by the ECE diagnostic in Pulse No's: 68730-68733 (B_0 = 3.3T) and 68734 (B_0 = 3.6T).